

# Contents

<b>1</b>	<b>Measurement of the CENNS with Cryogenic Bolometers in the RICOCHET experiment</b>	<b>1</b>
1.1	CE $\nu$ NS and the new physics	1
1.1.1	Neutrino/core elastic coherent scattering	1
1.1.2	The Atomic Nucleus	1
1.1.3	The Neutrino	2
1.1.4	CENNS and Standard Model	2
1.1.5	First Detection of CE $\nu$ NS	4
1.2	Search for New Low Energy Physics	4
1.2.1	Neutrino Sources	5
	Solar Neutrinos	5
	Terrestrial Neutrinos (geo-neutrinos)	6
	Production from Human Activity	6
1.2.2	Reactor Experiments	7
1.2.3	RICOCHET	8



## Chapter 1

# Measurement of the CENNS with Cryogenic Bolometers in the RICOCHET experiment

## 1.1 $\text{CE}\nu\text{NS}$ and the new physics

### 1.1.1 Neutrino/core elastic coherent scattering

A scattering phenomenon occurs when two particles interact during a collision. A scattering is considered to be elastic when the energies of the two particles is conserved through the collision, even though their momentum is not necessarily preserved. This work especially focuses on the elastic scattering between neutrinos and atomic nuclei. Even though the nucleus is an assembly of elementary particles, a coherent scattering occurs when the neutrino can interact with the nucleus as a whole as if it was a uniform object. When the scattering of a neutrino on a nucleus is coherent and elastic, it is defined as a Coherent Elastic Neutrino-Nucleus Scattering, shortened to  $\text{CE}\nu\text{NS}$  or CENNS. This physical phenomenon, described by Freedman in 1973 within the framework of the standard model, was experimentally measured for the first time in August of 2017 by the collaboration COHERENT installed near the spallation source at the Oak Ridge National Laboratory in the United States. Before getting to the heart of the matter, we can recall the various physical characteristics that will be discussed throughout this manuscript and present the scientific context of this work. We will therefore discuss the atomic nuclei, the neutrinos, the CENNS equations and the various experiments aimed at measuring this very scattering process.

### 1.1.2 The Atomic Nucleus

Rutherford's experience with gold leaf in 1909 provided valuable information for the development of Bohr's atomic model in 1913. Rutherford understood that the electrically positive charge of an atom is concentrated in the middle of the atom. Indeed, knowing that the matter is electrically neutral and that an atom has electrons (charged negatively) there are necessarily positive charges "somewhere". Bohr then designed an atomic model for the hydrogen that reminds us of a planetary system. There would be the nucleus at center and the electrons around it, only allowed to be on specific circular orbitals. Theoretical and experimental developments show us today that the electrons are not really on circular orbits but rather have a probability of presence described by combinations of spherical harmonics. Bohr's model for hydrogen is not fundamentally questioned and is still taught. Electrons are considered to orbit around the nucleus of positive charge. The latter can be either stable or unstable in the case of radioactive elements. This is an important fact, that an atom is not a fundamental object of modern physics: it is composed of nucleons (neutrons and protons), which are themselves composed of three quarks held together by the strong nuclear interaction mediated by gluons. The size of an

atom is of the order of  $0.1 \text{ nm} = 1 \times 10^{-10} \text{ m}$  which five order of magnitude larger than the size of its nucleus  $1 \text{ fm} = 1 \times 10^{-15} \text{ m}$ .

### 1.1.3 The Neutrino

The neutrino is one of the elementary particles of the Standard Model of Particle Physics. Technically it is said to be an electrically neutral lepton. There are three flavors of neutrinos each associated with a lepton: the electronic neutrino  $\nu_e$  is the equivalent of the electron  $e^-$ , the muonic neutrino  $\nu_\mu$  for the muons  $\mu^-$  and the tauic neutrino  $\nu_\tau$  for the tau  $\tau^-$ . The physicist Wolfgang Pauli was the first to postulate the existence of the neutrino in 1930. This new particle (at the time) helped to explain the continuous spectrum of the beta disintegration, which is a radioactive reaction in which a radionuclide emits an electron (or positron) and an (anti-)neutrino. The experimental confirmation will be made in 1952 by Cowan and Reines based on an idea by Wang Ganchang (1942), the first two were awarded the Nobel Prize for physics in 1995 for this discovery. A neutrino is only sensitive to the weak nuclear force and gravity. The latter is negligible in particle physics but holds impact on the larger scale of cosmology. Due to the short range of the weak interaction  $10^{-18} \text{ m}$  the neutrino has a very low probability of interaction with matter, which is formalized in particle physics as a weak cross-section. To have an order of magnitude in mind we can show that out of 10 billion neutrinos of 1 MeV that cross the Earth, only 1 will interact with matter. In the study of the CENNS process, no particular attention is brought on distinguishing neutrinos from anti-neutrinos as well as different flavors. Indeed, this scattering process is insensitive to these differences.

### 1.1.4 CENNS and Standard Model

It was in 1973 that Daniel Z. Freedman, a physicist currently at MIT, proposed the coherent elastic neutrino-nucleus scattering as a probe for weak interaction. In its description based on the standard particle physics model still under development at the time (it will take its current form in the mid-1970s) Freedman expresses the evolution rate of the effective cross-section of the neutrino-nucleus interaction as a function of the recoil energy of the nucleus:

$$\frac{d\sigma(E_\nu, E_R)}{dE_R} = \frac{G_f^2}{4\pi} Q_w^2 m_A \left(1 - \frac{m_A E_R}{2E_\nu^2}\right) F^2(E_R) \quad (1.1)$$

This equation shows that the evolution of the effective cross-section noted  $\sigma(E_\nu, \sigma E_R)$  depends on the neutrino energy  $E_\nu$  and recoil energy  $E_R$  of the nucleus as well as of the mass of the target nucleus  $m_A$  and its composition  $(N, Z)$ . Without going into the details of the theoretical calculations to obtain this expression, one can try to explain simply the different terms.

The Fermi coupling constant is measured experimentally by studying the life time of the muon (inversely proportional to  $G_f^2$ ). We can express this constant with the coupling constant of the weak interaction  $g_W$ , the mass  $m_W$  of the boson  $W$ , the speed of light  $c$  and the reduced Planck constant  $\hbar$  according to the equation:

$$G_f = \frac{\sqrt{2}}{8} \left(\frac{g_W}{m_W c^2}\right)^2 (\hbar c)^3 \sim 1.17 \times 10^{-5} \text{ GeV}^{-2} \quad (1.2)$$

The weak nuclear hypercharge  $Q_w$  is given by:

$$Q_w = N - Z(1 - 4 \sin^2 \theta_w) \quad (1.3)$$

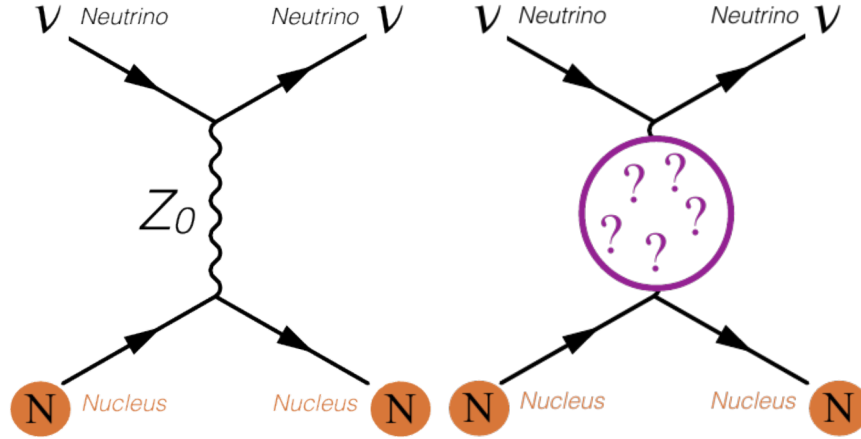


FIGURE 1.1: Feynman diagram of the CEvNS. On the left in the case of the standard model. To the right the same process within the framework of alternative theories.

It depends on the number of neutrons  $N$  and protons  $Z$  composing the nucleus. The term  $\theta_w$  is the mixing angle which is a parameter of the Weinberg-Salam theory of the electro-weak interaction (reunification of the theory of electromagnetism and weak interaction). The value of  $\sin^2 \theta_w$  is close to 0.24. Thus, in practice, the hypercharge simplifies to  $Q_w \simeq N$ . As described later in this work, the measurement of the  $\sin^2 \theta_w$  as a function of the transferred momentum would permit to probe for new physic in the electroweak sector.

The shape factor  $F$  is a function of the recoil energy that characterizes the loss of coherence at high transferred momentum. It is worth 1 for low recoil energies, so it is often neglected in very low energy regimes, and decreases with the recoil energy  $E_R$ .

The effective cross-section  $\sigma$  associated with the CENNS is obtained by integrating the equation 1.1 from  $E_R = 0$  to  $E_R^{max} = 2E_\nu^2 / (m_A + 2E_\nu)$ , the maximum recoil energy of the nucleus accessible for a given neutrino energy  $E_\nu$ . Its expression is:

$$\sigma \sim \frac{G_f^2 N^2}{4\pi} E_\nu^2 \quad (1.4)$$

which is proportional to the square of the number of neutrons  $N$  in the target nucleus and the energy of the neutrino thanks to the coherence of the interaction in case  $m_N \gg E_\nu$ .

The detection of CENNS is not done by directly measuring the cross-section of the particles that interact with the atomic nuclei of the detector. We measure the number of neutrinos having interacted with a nucleus according to the recoil energy of the latter. By doing this on a fairly wide range of recoil energy, we end up with what is called a energy spectrum of CENNS events. In this case, we will speak of CENNS spectrum, and of energy spectrum in the general case for different scattering processes. The expected differential CENNS event rate  $R$  is calculated from the differential cross-section by convolving with the incoming neutrino flux  $\Phi$ :

$$\frac{dR}{dE_r} = \mathcal{N} \cdot \int_{E_\nu^{min}} \Phi(E_\nu) \cdot \frac{d\sigma(E_\nu, E_r)}{dE_r} dE_\nu \quad (1.5)$$

In this equation,  $\mathcal{N}$  represents the number of target nuclei per mass unit. The minimum energy of a neutrino to induce a nuclear recoil is given by the relation  $E_\nu^{min} = \sqrt{m_N E_R / 2}$ .

A common representation of this type of interaction in particle physics is done with the help of Feynman diagrams. In this representation, the time flows from left to right and the distance between the particles is represented along the vertical axis. The mediator bosons are indicated with wavy lines. The figure 1.1 displays two Feynman diagram for the CENNS. The left diagram

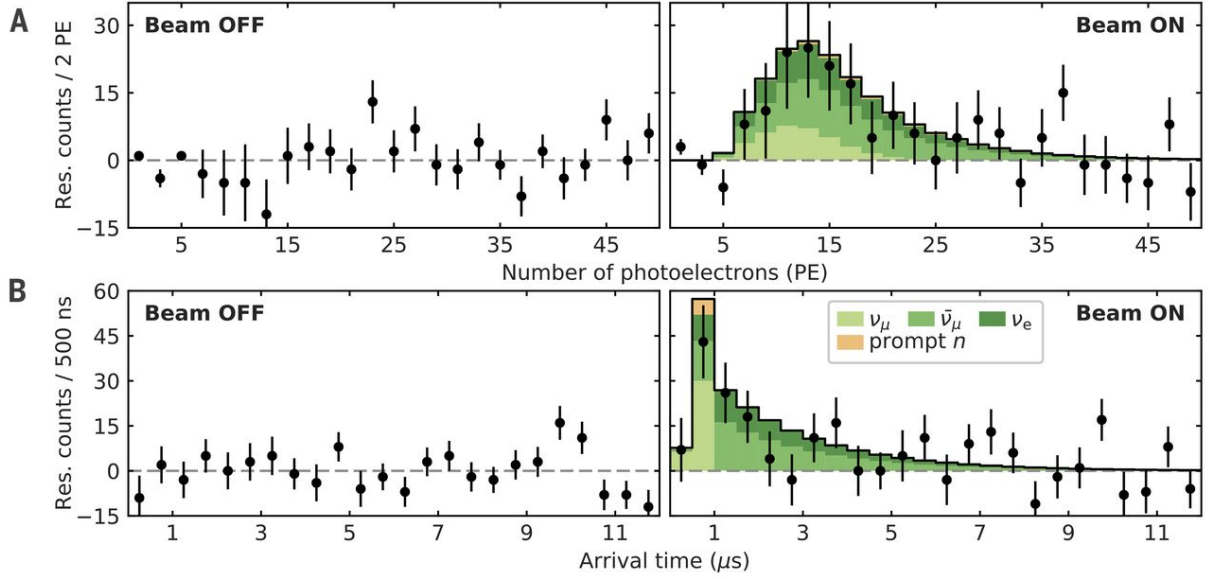


FIGURE 1.2: Experimental result of the COHERENT experiment at the SNS demonstrating unambiguously the existence of the CENNS.

corresponds to the CENNS following the usual standard model by having the the  $Z_0$  boson as the mediator of the weak interaction between the neutrino and the nucleus. The right diagram humbly presents the CENNS in the framework of alternative theories.

### 1.1.5 First Detection of $\text{CE}\nu\text{NS}$

The COHERENT collaboration was the first to observe experimentally and unambiguously the signature of the CENNS in August 2017. The technology used at that time was a 14.6 kg sodium-doped cesium iodide ( $\text{CsI}[\text{Na}]$ ) scintillator instrumented with photo-multipliers. The detector was located at a distance of 19.3 m from the neutrino source and had an energy detection threshold of 4.5 keV. The neutrino flux of average energy  $E_\nu = 30 \text{ MeV}$  used for this detection was produced with the so-called "pion-at-rest" method. It consists in taking advantage of the decay of positive pions, obtained after a controlled collision of a mercury atom with a proton, which leads to the production of neutrinos and anti-neutrinos. The proton source comes from the SNS (Spallation Neutron Source) located at the Oak Ridge National Laboratory in Oak Ridge, Tennessee (USA).

Scientists in the collaboration have detected an excess of CENNS-related events, shown in Figure 1.2, with a confidence of  $6.7\sigma$  compatible at  $1\sigma$  with the standard model. The uncertainty of the statistical study they estimate is 16 %. This first detection of CENNS is a result which proves the existence of this phenomenon which has been considered for years by some as purely hypothetical. It has made it possible to constrain models of new physics but the current data do not allow to study the theories expected in the lower energies such as the existence of new mediating bosons. This requires a source of lower energy neutrinos.

## 1.2 Search for New Low Energy Physics

A number of theories diverge significantly from the prediction of the standard model at low energy. Among them we can mention in particular :

- The existence of a new  $Z_0$  mediator bosons,

- The existence of an abnormally high magnetic moment of the neutrino,
- The existence of non-standard interactions.

There is an important scientific stake in making these low energy measurements to provide additional elements in the understanding of fundamental interactions but also to provide additional constraints for a large number of neutrino research projects. A precise measurement of the CENNS would, for example, make it possible to constrain multiples theoretical models.

However, to do new physics research with the CENNS process, the use of a suitable neutrino source is required. This source should have a known and adapted neutrino energy spectrum (typically  $E_\nu \approx 10 \text{ MeV}$ ). This will results in lowered recoil energies  $E_R$  in the detector which should be be enhanced with higher sensitivities to the signal. This upgrade in detector performances can only be reached by diminishing the volume of the detectors resulting in a loss of exposure. As such, the new source should produce a very high flux of neutrinos as to counter the inevitable loss of detector mass and obtain an equivalent CENNS event rate.

Additionally, various technical and practical considerations are taken into account: possibility of interruption of the flow (or pulsed flow) for background rejection (as in the case of COHERENT for example), minimum accessible source/detector distance, ease of access and installation, regulations and availability of infrastructure.

### 1.2.1 Neutrino Sources

There are many sources of neutrinos because the radioactive decay processes that generate them are very common in nature. This subsection discusses some common neutrino sources and their characteristics regarding the search for the CENNS. Neutrinos out of experimental range such as those composing the neutrino diffuse background (the analogue of the neutrino diffuse cosmological background for neutrinos) will not be discussed. The resting pion method used by COHERENT will not be recalled as it has already been presented and is not a viable solution for the search for new low energy physics because of the too large energy of the emitted neutrinos.

#### Solar Neutrinos

Thermonuclear fusion reactions take place in the heart of stars. During these reactions, low energy neutrinos (a few MeV) are emitted. They escape from their original star without great difficulty thanks to their low effective cross-section. The process responsible for about 85 % of the neutrino emission of the Sun, is the fusion of two protons  $p$  into a  $^2\text{H}$  deuterium (heavy hydrogen) nucleus, an anti-electron  $e^+$  (otherwise known as positron) and an electronic neutrino  $\nu_e$ :



For this specific reaction the energy of the emitted neutrinos is in the order of  $\mathcal{O}(100)$  kiloeV. It should be noted, however, that there are other reactions of a different nature producing neutrinos within the sun. The figure 1.3 displays on the left, the simulated spectrum of the neutrino flux as seen from Earth associated with these different processes. Taking all energies together, from the Earth, the flux of solar neutrinos is of the order of  $7 \times 10^{10} \text{ cm}^{-2}\text{s}^{-1}$  which is relatively small and makes the detection of solar neutrinos very difficult.

Despite this difficulty, large experiments, such as Borexino located in the underground laboratory of the Gran Sasso in Italy, are able to measure this solar neutrino spectrum as seen on the right subplot of figure 1.3. However, for a CENNS precision measurement experiment the sun is clearly not a relevant source because even if the energy of some neutrinos is low enough for probing new physics, it is not a relevant source of energy as the flux remains far too low and would require a huge volume (mass) of detector. Another negative point is that it is not

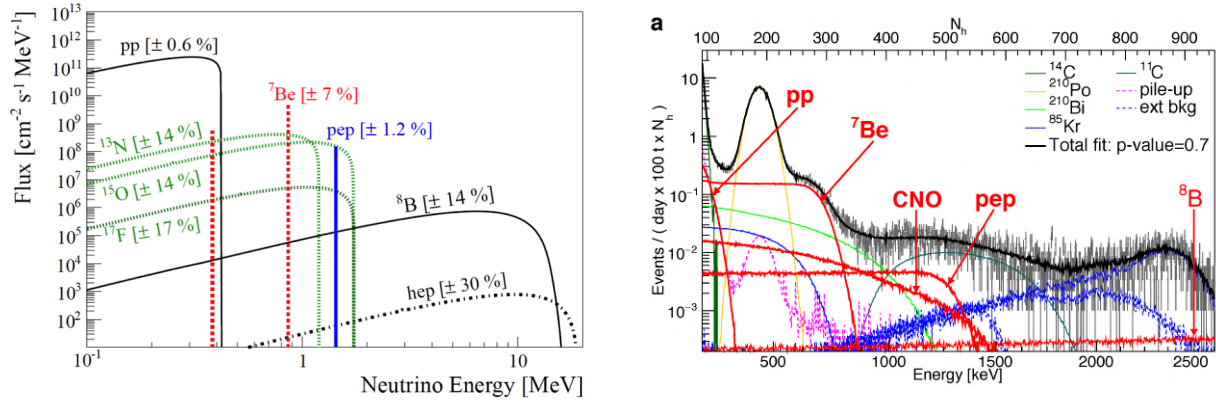


FIGURE 1.3: Solar neutrino spectrum. On the left, simulated spectra of solar neutrinos seen from the Earth associated with the different fusion reaction. On the right, solar neutrino spectrum and its components measured by the Borexino experiment at the Gran Sasso in Italy.

possible to turn off the source to identify the background noise. Indeed, the solar neutrino flux is constant and crosses the Earth to reach the detector without difficulty.

### Terrestrial Neutrinos (geo-neutrinos)

Our own planet, the Earth, emits neutrinos through natural radioactivity processes. Neutrinos resulting from these radioactive processes are numerous, it is estimated that the flow of neutrinos of origin geologic surface of the earth around  $1 \times 10^6 \text{ cm}^{-2}\text{s}^{-1}$ . This flux of geo-neutrinos is low and is coupled with a wide distribution in energy. Consequently, they are very difficult to detect because of the background of neutrinos from extraterrestrial and human origin. Nevertheless some experiments try to carry out geo-neutrino measurements for the information they would allow us to obtain on the Earth and in particular at the level of the Earth's core. The same large-scale experiment Borexino claims to have recently detected 53 events attributable to geo-neutrinos. For reasons similar to solar neutrinos, geo-neutrinos are not relevant in view of the current knowledge for CENNS precision measurement.

### Production from Human Activity

Humans are capable of producing neutrinos in controlled physical processes. In particle accelerators, for example, it is not uncommon to produce neutrinos with energies of up to 100 GeV. The most intense man-made source of low-energy neutrinos are the nuclear fission power plants. However, the main objective of these power generation plants is not the production of neutrinos, which consists in a very abundant by-product of the electricity production. The flow of neutrinos emitted by a standard nuclear power plant 10 m from the reactor is approximately equal to  $2 \times 10^{15} \text{ cm}^{-2}\text{s}^{-1}$ , for an average neutrino energy of 4 MeV. Nuclear fission reactors offer a range of energy compatible with the research of new physics as envisioned by RICOCHET, the neutrino flux is among the most important and in addition to that it is possible to take advantage of unit outages to measure background noise. For this last point the subtraction background noise is not as optimal as with a pulsed source if the background noise is not stationary on the time scales represented by the combustion of a fuel rod but it is always an interesting plus to gain in measurement accuracy.



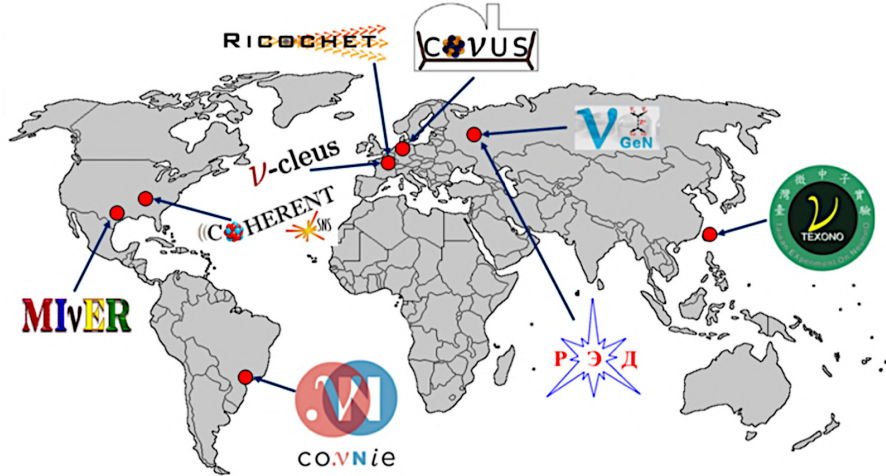


FIGURE 1.4: Main experiences of CEvNS in the world today (2020).

Experiment	(Detector Material) @ Location	Reference
NuGEN	(Ge) @ Kalinin Reactor (Russie)	[10]
CONUS	(Ge) @ Brokdorf (Allemagne)	[11]
TEXONO	(Ge) @ Kuo-Sheng Reactor (Taiwan)	[12]
CONNIE	(Si) @ Angra Reactor (Brésil)	[13]
RED100	(Xe) @ Kalinin Reactor (Russie)	[14]
MINER	(GeSi) @ Nuclear Science Center (USA)	[15]
NU-CLEUS	(CaWO <sub>4</sub> , Al <sub>2</sub> O <sub>3</sub> ) @ Chooz (France)	[16]
RICOCHET	(Ge, Zn, Al, (Si)) @ ILL (France)	[17]

TABLE 1.1: Presentation of CENNS experiments associated with a nuclear reactor: materials used for detection @ localization. In red are represented the cryogenic experiments with a very low detection threshold for the research of new physics. The RICOCHET experiment is the only one to propose a detector capable of discriminating between nuclear and electronic recoils.

### 1.2.2 Reactor Experiments

The strong potential of nuclear power plants as sources of neutrinos has led a small number of CENNS experiments to be installed close to a reactor core around the world. The main experiments searching for the the CENNS near nuclear reactors are identified on the atlas displayed in figure 1.4 and listed in the table 1.1 with their material used for their crystalline detector and their localization.

The CENNS experiments near a reactor would allow the estimation the Weinberg angle  $\theta_w$  at low energies. Figure 1.5 shows the prediction of the standard model (blue line) for this parameter and the zone of the parameter space accessible by the CENNS experiments (green zone) which still remains largely unexplored. The estimation of this parameter with different physical processes is also very important to identify incompatibilities and allow the scientific community to go beyond the current theoretical model.

In view of the number of CENNS experiments, we can expect this precision measurement within a few years. What is uncertain is whether this scientific result will deviate from the standard model at low-energy scale or confirm this theory. The "cooperation" at work between all these collaborations and with dark matter experiments such as EDELWEISS favors rapid developments and technological improvements.

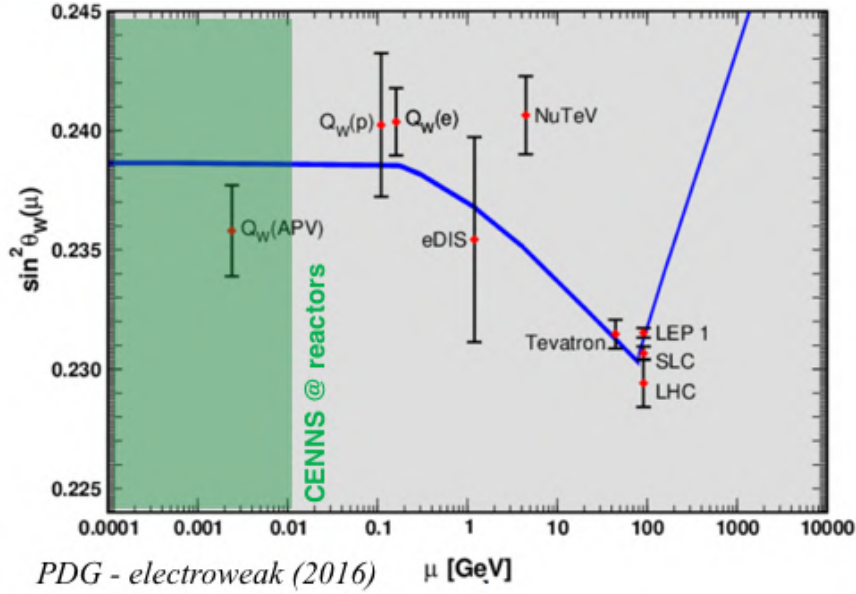


FIGURE 1.5: Measurements of the Weinberg angle as a function of the impulse (or transferred momentum). The blue curve is the prediction of the standard model for different processes and experiments. The green area shows the area accessible with a precision measurement of the CENNS spectrum near a nuclear reactor.

### 1.2.3 RICOCHET

RICOCHET is a CENNS experiment led by the members of the MANOIR team at the *Institut de Physique des deux Infinis* (IP2I) of Lyon, which brings together some fifty researchers, technicians and engineers through various laboratories and universities in France, Russia and the United States. RICOCHET aims at measuring the CENNS spectrum with a statistical accuracy of 1 % after one year of taking data. With this objective, the detection CENNS with low energy neutrinos (a few MeV) with an accuracy of at least  $5\sigma$ , like the COHERENT experiment, will be reached within a week of operation. It should be noted that the targeted accuracy is far superior to that obtained by COHERENT. To achieve these scientific objectives the RICOCHET device is composed of a cryogenic system, a shielding to limit sources of unwanted noise and the CRYOCUBE detector. It will be installed in 2022 at the Laue Institute Langevin (ILL) in Grenoble, France. The ILL hosts a 58 MW fission research nuclear reactor. A numerical modeling of RICOCHET at ILL and the implementation scheme near the reactor core are presented in figure 1.6.

The CRYOCUBE detector will be at only 8 m from the core of the nuclear reactor with a power of 58 MW which will produce a neutrino flux of  $10^{12} \text{ cm}^{-2} \text{ s}^{-1}$ . The CRYOCUBE will be cool down close to the absolute zero at cryogenic temperatures comprised between 5 and 20 mK, in order to be able to measure minute temperature rises caused by the neutrinos during their interaction with the nuclei that make up the detector's target material.

The cryogenic detector load will be protected from external radiation by a thick layer of lead and borated poly-ethylene shielding weighting more than 15 tons and an active cosmic particle rejection device designated as "veto muon". The objective of this shielding strategy is prevent as much as possible any unwanted diffusion processes in the experimental data which would increase the signal-to-noise ratio and significantly hurt the chances of detecting signs of new physics.

The incident neutrino flux on the location of the CRYOCUBE at the ILL site was estimated and the Manoir team has precisely simulated the expected CENNS spectrum according to different theoretical models considered and taking into account the different background noises. On

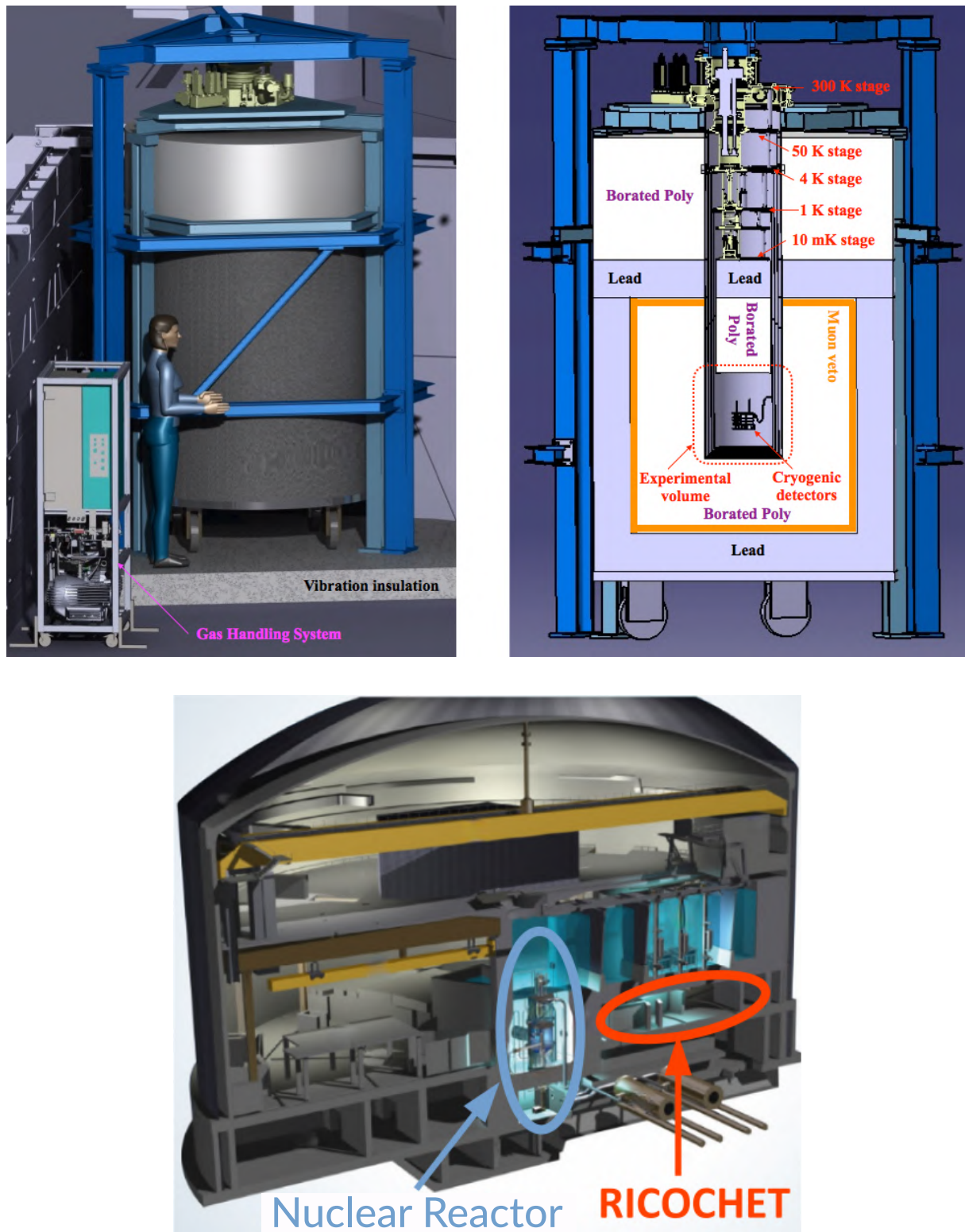


FIGURE 1.6: On the top left Installation of RICOCHET at ILL, 3D modeling. On the top right, View in cryostat cut. At the bottom, location of the RICOCHET cryostat within the ILL nuclear reactor. The water pool above the location of RICOCHET provides protection against cosmic particles.

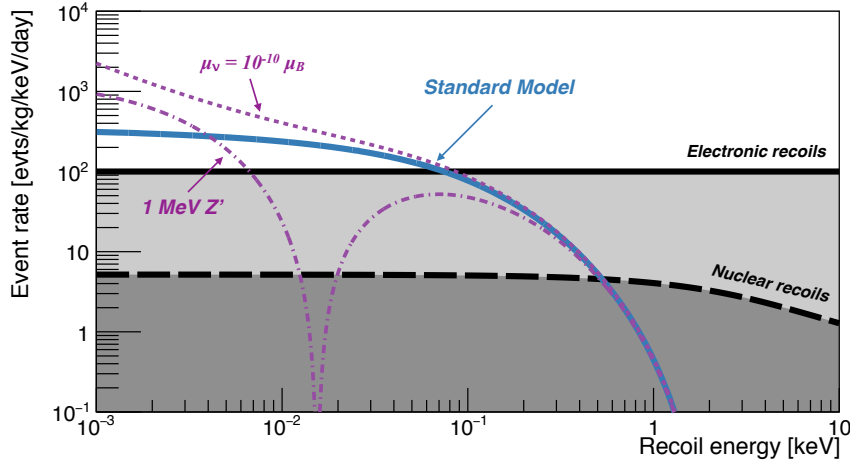


FIGURE 1.7: On the left, Simulation of the background noise on the CENNS spectrum for RICOCHET at the ILL. The radioactive background noise is represented as its two components inducing electronic recoils in light grey and inducing nuclear recoils in dark grey.

the left subplot of figure 1.7, we see the prediction of the standard model (in blue) and the assumed effect of two alternative theories: the existence of an abnormally high neutrino moment (violet, fine dotted line) or of a new particular  $Z'$  boson (violet, dashed line). The background noise, of electronic or nuclear origin, is represented in grey and is both almost uniform in the energy range considered.

This numerical simulation allows to define the specifications of RICOCHET so that the CENNS spectrum is measured specifically in the region of interest for the new physics. From the spectra associated with two exotic physics scenario in figure 1.7, we see that we need a low enough detection threshold in recoil energy. Otherwise, we will not be able to see the deviations from the standard model or even the CENNS itself.

We can notice that the spectrum is given in events/keV/kg/d and therefore to have a sufficient statistic it is necessary to find an interesting ratio of detector mass over data acquisition time. Indeed having an ultra massive detector represents a real technical challenge. One can quote for example the dark matter research experiment XENON1T which uses a detector whose total mass is greater than one ton and its version in development XENONnT which aims to go even further in terms of mass. This detector technology, based on a liquefied noble gas, is not the most efficient for the CENNS but above all requires a large experimental volume that is difficult to obtain near a nuclear reactor. Other technologies such as super-K or Borexino experiments would be theoretically possible but the experimental volume would remain an impossible constraint to reconcile with the proximity to the nuclear reactor. The opposite approach consists in taking a low detector mass, which easier to install, operate, analyze and protect from external background noise, and collecting experimental data for a long time. In theory there would be no problem to this, but in practice the non-stationarity of the noise, the volume of the data, the time to analyze this data and the time of experience (mobilization of human resources, technical, infrastructure, ...) make the task very difficult. There is therefore a compromise to be made between the mass of the detector and the desired duration of data acquisition for a given number of CENNS events.

The exposure of the detector, its mass multiplied by the experiment time) in  $\text{kg} \cdot \text{d}$ , is not



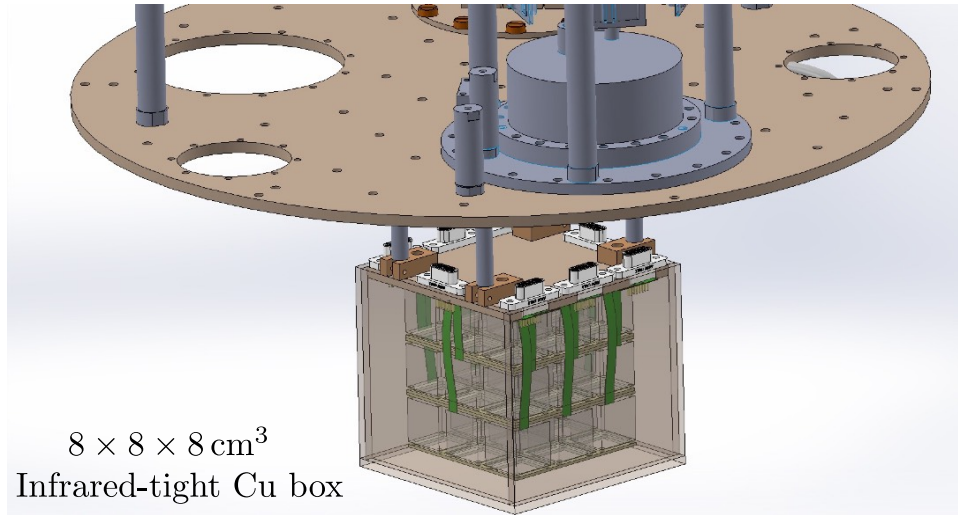


FIGURE 1.8: 3D model of the CRYOCUBE installed at the coldest stage of its cryostat. We can see by transparency the 27 germanium crystals of 38g electrically connected to the systems of acquisition by the green cables.

the only parameter to be considered, it is necessary to have sufficient sensitivity to measure the minute variations in temperature generated by the interaction of a neutrino with matter and to be able to differentiate between nuclear and electronic recoils in order to increase the signal-to-noise ratio (as suggested by numerical simulation).

To carry out this identification of neutrino recoils, one way to do this is to measure the temperature increase induced by a deposit of energy while measuring the electron-hole pairs created in the semiconductor material that serves as a target for coherent elastic scattering. This double energy measurement is described later in the section ??.

Specifically, a detector with the following characteristics would be required:

- Detection threshold / energy resolution:  $E_R \sim 50 \text{ eV} / \sigma(E_R) \sim 10 \text{ eV}$
- Ability to discriminate between electronic and nuclear recoil with thermometer + electrodes for electronic noise rejection with semiconductor material
- Mass of the detector:  $m_d \sim 1 \text{ kg}$  with a flux of  $10^{12} \text{ cm}^{-2}\text{s}^{-1}$  to have about ten of CENNS events per day

To meet these specifications, the members of the RICOCHET collaboration are developing an innovative detector called CRYOCUBE which is presented in the figure 1.8. It will be composed of 27 germanium crystals of 38 g equipped with a heat measurement channel and an ionization measurement channel for discrimination purpose.